

Multichannel quantum-defect theory for slow atomic collisions

Bo Gao,^{1,*} Eite Tiesinga,² Carl J. Williams,² and Paul S. Julienne²

¹*Department of Physics and Astronomy, University of Toledo, Toledo, Ohio 43606, USA*

²*Atomic Physics Division, National Institute of Standards and Technology, Gaithersburg, Maryland 20899, USA*

(Received 8 August 2005; published 28 October 2005)

We present a multichannel quantum-defect theory for slow atomic collisions that takes advantages of the analytic solutions for the long-range potential and both the energy and angular momentum insensitivities of the short-range parameters. The theory provides an accurate and complete account of scattering processes, including shape and Feshbach resonances, in terms of a few parameters such as the singlet and triplet scattering lengths. As an example, results for ^{23}Na - ^{23}Na scattering are presented and compared to close-coupling calculations.

DOI: [10.1103/PhysRevA.72.042719](https://doi.org/10.1103/PhysRevA.72.042719)

PACS number(s): 34.10.+x, 03.75.Nt, 32.80.Pj

I. INTRODUCTION

Slow atomic collisions are at the very foundation of cold-atom physics, since they determine how atoms interact with each other and how this interaction might be manipulated [1,2]. While substantial progress has been made over the past decade [3], there are still areas where the existing theoretical framework is less than optimal. For example, all existing numerical methods may have difficulty with numerical stability in treating ultracold collisions in partial waves other than the s wave, because the classically forbidden region grows infinitely wide as one approaches the threshold. This difficulty becomes a serious issue when there is a shape resonance right at or very close to the threshold, as the usual argument that the s -wave scattering dominates would no longer be applicable. Another area where a more optimal formulation is desirable is analytic representation. Since much of our interest in cold atoms is in complex three-body and many-body physics, a simple, preferably analytical representation of cold collisions would not only be very helpful to experimentalists, but also make it much easier to incorporate accurate two-body physics in theories for three- and many-atom systems. Existing formulations of cold collisions provide little analytical results especially in cases, such as the alkali-metal atoms, where the atomic interaction is complicated by hyperfine structures. Furthermore, whatever analytic results that we do have have been based almost exclusively on the effective-range theory [4], the applicability of which is severely limited by the long-range atomic interaction [5,6].

Built upon existing multichannel quantum-defect theories that are based either on free-particle reference functions or on numerical solutions for the long-range potential [7–12], we present here a multichannel, angular-momentum-insensitive, quantum-defect theory (MAQDT) that overcomes many of the limitations of existing formulations. It is a generalization of its single-channel counterpart [13–15] and takes full advantage of both the analytic solutions for the

long-range potential [16,17] and the angular momentum insensitivity of a properly defined short-range K matrix K^c [13,15]. We show that as far as K^c is concerned, the hyperfine interaction can be ignored and the frame transformation [9,10,18–20] applies basically exactly. This conclusion *greatly* simplifies the description of any atomic collision that involves hyperfine structures. In the case of a collision between any two alkali-metal atoms in their ground state, whether they are identical or not, it reduces a complex multichannel problem to two *single-channel* problems. This property, along with the energy and angular momentum insensitivity of K^c [13,15], leads to an accurate and *complete* characterization of slow collisions between any two alkali-metal atoms, including shape resonances, Feshbach resonances, and practically all partial waves of interest, and over an energy range of hundreds of millikelvins, by four parameters for atoms with identical nuclei, and five parameters for different atoms or different isotopes of the same atom. To be more specific, the four parameters can be taken as the singlet s -wave scattering length a_{0S} , the triplet s -wave scattering length a_{0T} , the C_6 coefficient for the long-range van der Waals potential $-C_6/r^6$, and the atomic hyperfine splitting ΔE_a^{HF} (the reduced mass μ , which is also needed, is not counted as a parameter since it is always fixed and well known). For different atoms or different isotopes of the same atom, we need another hyperfine splitting for a total of five parameters. These results also prepare us for future analytic representations of multichannel cold collisions, when we restrict ourselves to a smaller range of energies.

II. MAQDT

An N -channel, two-body problem can generally be described by a set of wave functions

$$\psi_j = \sum_{i=1}^N \Phi_i F_{ij}(r)/r. \quad (1)$$

Here Φ_i are the channel functions describing all degrees of freedom other than the interparticle distance r and $F_{ij}(r)$ satisfies a set of close-coupling equations

*Electronic address: bgao@physics.utoledo.edu; <http://bgaowww.physics.utoledo.edu>

$$\left[-\frac{\hbar^2}{2\mu} \frac{d^2}{dr^2} + \frac{\hbar^2 l_i(l_i+1)}{2\mu r^2} - E \right] F_{ij} + \sum_{j=1}^N V_{ij}(r) F_{ij} = 0, \quad (2)$$

where μ is the reduced mass, l_i is the relative angular momentum in channel i , E is the total energy, and V_{ij} is the representation of the interparticle potential in the set of chosen channels (see, e.g., Ref. [9] for a diatomic system with hyperfine structures).

Consider now a class of problems for which the potential at large distances ($r \geq r_0$) is of the form of

$$V_{ij}(r) = (E_i - C_{n_i}/r^{n_i}) \delta_{ij}, \quad (3)$$

in the fragmentation channels that diagonalize the long-range interactions. Here $n_i > 2$ and E_i is the threshold energy associated with a fragmentation channel i . As an example, for the scattering of two alkali-metal atoms in their ground state, the fragmentation channels in the absence of any external magnetic field are characterized by the *FF* coupling of reference [9], differences in threshold energies originate from atom hyperfine interaction, $n_i=6$ corresponds to the van der Waals interaction, and r_0 , with an order of magnitude around 30 a.u., corresponds to the range of exchange interaction.

Before enforcing the physical boundary condition (namely, the condition that a wave function has to be finite everywhere) at infinity, Eq. (2) has N linearly independent solutions that satisfy the boundary conditions at the origin. For $r \geq r_0$, one set of these solutions can be written as

$$\psi_j^c = \sum_{i=1}^N \Phi_i (f_i^c \delta_{ij} - g_i^c K_{ij}^c) / r. \quad (4)$$

Here f_i^c and g_i^c are the reference functions for the long-range potential $-C_{n_i}/r^{n_i}$ in channel i at energy $\epsilon_i = E - E_i$. They are chosen such that they are independent of both the channel kinetic energy ϵ_i and the relative angular momentum l_i at distances much smaller than the length scale $\beta_{n_i} = (2\mu C_{n_i} / \hbar^2)^{1/(n_i-2)}$ associated with the long-range interaction (see Appendix A and Refs. [13,15]).

Equation (4) defines the short-range K matrix K^c . It has a dimension equal to the total number of channels, N , and encapsulates all the short-range physics. The K^c matrix can either be obtained from numerical calculations (see Appendix B) or be inferred from other physical quantities such as the singlet and triplet scattering lengths, as discussed later in the article.

At energies where all N channels are open, the solutions given by Eq. (4) already satisfy the physical boundary conditions at infinity. Using the asymptotic behaviors of reference functions f^c and g^c at large r (see Appendix A and Ref. [16]), it is easy to show from Eq. (4) that the physical K matrix, defined by Eqs. (4) and (5) of Ref. [9], is an $N \times N$ matrix given in terms of K^c by

$$K(E) = - (Z_{fg}^c - Z_{gg}^c K^c) (Z_{ff}^c - Z_{gf}^c K^c)^{-1}. \quad (5)$$

Here Z_{fg}^c , Z_{gg}^c , Z_{ff}^c , and Z_{gf}^c are $N \times N$ diagonal matrices with diagonal elements given by $Z_{fg}^{c(n_i)}(\epsilon_i, l_i)$, $Z_{gg}^{c(n_i)}(\epsilon_i, l_i)$, $Z_{ff}^{c(n_i)}(\epsilon_i, l_i)$, and $Z_{gf}^{c(n_i)}(\epsilon_i, l_i)$, respectively (see Appendix A and Refs. [14,16]). Equation (5) is of the same form as its

single-channel counterpart [13,14], except that the relevant quantities are now matrices and K^c is generally *not* diagonal.

At energies where N_o of the channels are open ($\epsilon_i > 0$, for $i \in o$) and $N_c = N - N_o$ of the channels are closed ($\epsilon_i < 0$, for $i \in c$), the physical boundary conditions at infinity lead to N_c conditions that reduce that number of linearly independent solutions to N_o [9,10,21]. The asymptotic behavior of these N_o solutions gives the $N_o \times N_o$ physical K matrix

$$K(E) = - (Z_{fg}^c - Z_{gg}^c K_{eff}^c) (Z_{ff}^c - Z_{gf}^c K_{eff}^c)^{-1}. \quad (6)$$

Here Z_{fg}^c , Z_{gg}^c , Z_{ff}^c , and Z_{gf}^c are $N_o \times N_o$ diagonal matrices with diagonal elements given by the corresponding Z^c matrix element for all open channels, and we have defined the effective K^c matrix for the open channels, K_{eff}^c , to be

$$K_{eff}^c = K_{oo}^c + K_{oc}^c (\chi^c - K_{cc}^c)^{-1} K_{co}^c. \quad (7)$$

Here χ^c is an $N_c \times N_c$ diagonal matrix with elements $\chi^{c(n_i)}(\epsilon_i, l_i)$ (see Appendix A and Refs. [13,16]) for all closed channels. K_{oo}^c , K_{oc}^c , K_{co}^c , and K_{cc}^c are submatrices of K^c corresponding to open-open, open-closed, closed-open, and closed-closed channels, respectively.

All on-the-energy-shell scattering properties can be derived from the physical K matrix. In particular, the physical S matrix is given by [9]

$$S(E) = [I + iK(E)][I - iK(E)]^{-1}, \quad (8)$$

where I represents a unit matrix. From the S matrix, the scattering amplitudes, the differential cross sections, and other physical observables associated with scattering can be easily deduced [9].

It is worth noting that Eq. (6) preserves the form of Eq. (5). Thus the effect of closed channels is simply to introduce an energy dependence, through χ^c , into the effective K^c matrix K_{eff}^c for the open channels. In particular, the bare (unshifted) locations of Feshbach resonances, if there are any, are determined by the solutions of

$$\det[\chi^c(E) - K_{cc}^c] = 0. \quad (9)$$

They are locations of would-be bound states if the closed channels are not coupled to the open channels. The same equation also gives the bound spectrum of true bound states at energies where all channels are closed.

This completes our summary of MAQDT. It is completely rigorous with no approximations involved. The theory is easily incorporated into any numerical calculations (see Appendix B). The difference from the standard approach is that one matches the numerical wave function to the solutions of the long-range potential to extract K^c , instead of matching to the free-particle solutions to extract K directly. This procedure converges at a much smaller $r=r_0$, the range of the exchange interaction, than methods that match to the free-particle solutions. Furthermore, since the propagation of the wave function from r_0 to infinity is done analytically, through the Z^c matrix for open channels and the χ^c function for closed channels, there is no difficulty in treating shape resonances right at or very close to the threshold. This improved convergence and stability does not, however, fully illustrate the power of MAQDT formulation and is not the focus of this article.

Instead, we focus here on the simple parametrization of slow atomic collisions with hyperfine structures made possible by MAQDT. The result also lays the ground work for future analytic representations of cold collisions.

III. SIMPLIFIED PARAMETRIZATION WITH A FRAME TRANSFORMATION

Equations (5)–(7) and (9) already provide a parametrization of slow-atom collisions and diatomic bound spectra in terms of the elements of the K^c matrix. For alkali-metal atoms in their ground state, where the multichannel nature arises from the hyperfine interaction, or a combination of hyperfine and Zeeman interactions for scattering in a magnetic field, this parametrization can be simplified much further by taking advantage of a frame transformation [9,10,18–20].

At energies comparable to, or smaller than, the atomic hyperfine and/or Zeeman splitting, one faces the dichotomy that the hyperfine and/or Zeeman interaction, while weak compared to the typical atomic interaction energy, is sufficiently strong that the physical K matrix changes significantly over a hyperfine splitting. (This is reflected in the very existence of Feshbach resonances [1,2] and states with binding energies comparable to or smaller than the hyperfine splitting.) As a result, the frame transformation does not apply directly to the physical K matrix itself and is generally a bad approximation even for the K^0 matrix of Ref. [9]. It was this recognition that first motivated the solutions for the long-range potentials [16,17].

This dichotomy is easily and automatically resolved with the introduction of the short-range K matrix K^c . The solution is simply to ignore the hyperfine and/or Zeeman interaction only at small distances and treat it exactly at large distances. For $r < r_0$, the atomic interaction is of the order of the typical electronic energy. Thus, as far as K^c , which converges at r_0 , is concerned, the hyperfine and/or Zeeman interaction can be safely ignored. In this approximation, the K^c matrix in the fragmentation channels can be obtained from the K^c matrix in the condensation channels—namely, the channels that diagonalize the short-range interactions—by a frame transformation.

For simplicity, we restrict ourselves here to the case of zero external magnetic field, although the theory can readily be generalized to include a magnetic field. The fragmentation channels are the FF coupled channels characterized by quantum numbers [9]

$$(\alpha_1 L_1 S_1 J_1 I_1 F_1)_A (\alpha_2 L_2 S_2 J_2 I_2 F_2)_B FITM_T,$$

where F results from the coupling of F_1 and F_2 ; l is the relative orbital angular momentum of the center-of-masses of the two atoms. T represents the total angular momentum, and M_T is its projection on a space-fixed axis [9].

Provided that the *off-diagonal* second-order spin-orbital coupling [22] can be ignored, a good approximation for lighter alkali-metal atoms, or more generally, for any physical processes that are allowed by the exchange interaction, the condensation channels can be taken as the LS coupled channels characterized by quantum numbers [9]

$$(\alpha_1 L_1 S_1 I_1)_A (\alpha_2 L_2 S_2 I_2)_B L I L S K I T M_T,$$

where $\mathcal{L} = \mathbf{L} + \mathbf{I}$ is the total orbital angular momentum. $\mathbf{S} = \mathbf{S}_1 + \mathbf{S}_2$ is the total electron spin. $\mathbf{I} = \mathbf{I}_1 + \mathbf{I}_2$ is the total nuclear spin. And $\mathbf{K} = \mathcal{L} + \mathbf{S}$ is the total angular momentum excluding nuclear spin.

Ignoring hyperfine interactions, as argued earlier, the K^c matrix in FF -coupled channels, labeled by index i or j , is related to the K^c matrix in LS -coupled channels, labeled by index α or β , by a frame transformation [9]:

$$K_{ij}^c = \sum_{\alpha\beta} U_{i\alpha} K_{\alpha\beta}^{c(LS)} U_{j\beta}, \quad (10)$$

where $K^{c(LS)}$ is the K^c matrix computed in the LS coupling *with the hyperfine interactions ignored*. The most general form of frame transformation $U_{j\beta}$ is given by Eq. (49) of Ref. [9]. For collisions between any two atoms with zero orbital angular momentum $L_1 = L_2 = L = 0$, including of course any two alkali-metal atoms in their ground states, the frame transformation simplifies to

$$U_{i\beta}(T) = \delta_{i|\beta} (-1)^{F_i + S_{\beta} + I_{\beta}} [F_{1i}, F_{2i}, F_i, S_{\beta}, K_{\beta}, I_{\beta}]^{1/2} \times \begin{Bmatrix} F_i & l_i & T \\ K_{\beta} & I_{\beta} & S_{\beta} \end{Bmatrix} \begin{Bmatrix} S_1 & S_2 & S_{\beta} \\ I_1 & I_2 & I_{\beta} \\ F_{1i} & F_{2i} & F_i \end{Bmatrix}, \quad (11)$$

for atoms with different nuclei. Here $[a, b, \dots] \equiv (2a+1)(2b+1)\dots$. For two atoms with identical nuclei, the same transformation needs to be multiplied by a normalization factor [9]:

$$U_{\{i\}\{\beta\}} = \{1 + \delta(\alpha_2 L_2 S_2, \alpha_1 L_1 S_1) [1 - \delta(J_{2i} F_{2i}, J_{1i} F_{1i})]\}^{1/2} \times U_{i\beta}. \quad (12)$$

We emphasize that to the degree that the hyperfine interaction in a slow atomic collision can be approximated by *atomic* hyperfine interactions, as has always been assumed [2], the frame transformation given by Eq. (10) should be regarded as *exact*. If the hyperfine interaction inside r_0 , the range of the exchange interaction, cannot be ignored, the true molecular hyperfine interaction [23] would have to be used. Inclusion of *atomic* hyperfine interactions inside r_0 is simply another approximation, and an unnecessary complication, which is of the same order of accuracy as ignoring it completely. In other words, any real improvement over the frame transformation has to require a better treatment of *molecular hyperfine interactions* [23]. A similar statement is also applicable to the Zeeman interaction.

The applicability of the frame transformation greatly simplifies the description of any slow atomic collision with hyperfine structures. For alkali-metal atoms in their ground state and ignoring off-diagonal second-order spin-orbital coupling [22], it reduces a complex multichannel problem to two single-channel problems, one for the singlet $S=0$ and one for the triplet $S=1$, with their respective single-channel K^c [13,14] denoted by $K_S^c(\epsilon, l_i)$ and $K_T^c(\epsilon, l_i)$, respectively. The K^c matrix in the LS coupling, $K^{c(LS)}$, is diagonal with diagonal elements given by either K_S^c or K_T^c [9]. Ignoring the energy and the angular momentum dependences of $K_S^c(\epsilon, l_i)$

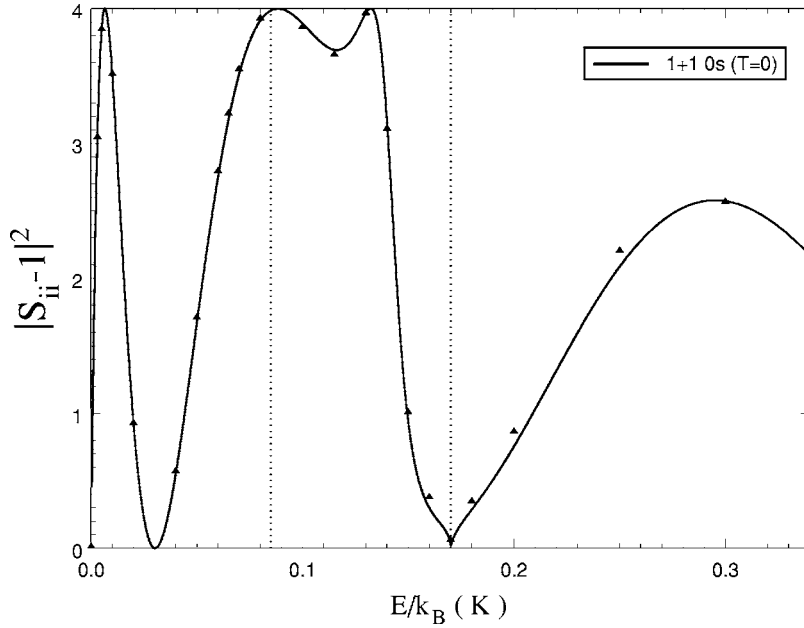


FIG. 1. $|S_{ii}-1|^2$, where S_{ii} is an S -matrix element, for the s -wave elastic scattering of two ^{23}Na atoms in channel $[\{F_1=1, F_2=1\}F=0, l=0, T=0]$, as a function of E/k_B , where k_B is the Boltzmann constant. The vertical lines identify the locations of thresholds for $\{F_1=1, F_2=2\}$ and $\{F_1=2, F_2=2\}$ channels. Solid line: results of a four-parameter MAQDT parametrization. Points: results of close-coupling calculations.

and $K_7^c(\epsilon, l_i)$ [13,15], they become simply two parameters $K_S^c=K_5^c(0,0)$ and $K_T^c=K_7^c(0,0)$, which are related to the singlet and triplet s -wave scattering lengths by [24]

$$a_0/\beta_n = \left[b^{2b} \frac{\Gamma(1-b)}{\Gamma(1+b)} \right] \frac{K^c(0,0) + \tan(\pi b/2)}{K^c(0,0) - \tan(\pi b/2)}, \quad (13)$$

where $b=1/(n-2)$ with $n=6$ for alkali-metal scattering in the ground state. With $K^{c(LS)}$, and therefore K^c , being parametrized by two parameters, a complete parametrization of alkali-metal scattering requires only two, or three, more parameters including C_6 , which determined the length and energy scales for the long-range interaction, and the atomic hyperfine splitting ΔE_a^{HF} , which characterizes the strength of atomic hyperfine interaction and also determines the channel energies.

We note here that our formulation ignores the weak magnetic dipole-dipole interaction [22,25]. It is important only for processes, such as the dipolar relaxation, that are not allowed by the exchange interaction. Such processes can be incorporated perturbatively after a MAQDT treatment [11]. We also note that for processes, such as the spin relaxation of Cs, for which the off-diagonal second-order spin-orbital coupling is important [22,26], a different choice of condensation channels, similar to the JJ -coupled channels of Ref. [9], would be required. The resulting description is similar conceptually, but involves more parameters [22,26].

IV. SAMPLE RESULTS FOR SODIUM-SODIUM SCATTERING

As an example, Figs. 1–3 show the comparison between close-coupling calculations and a four-parameter MAQDT parametrization for slow atomic collisions between a pair of ^{23}Na atoms in the absence of external magnetic field. The points are the close-coupling results using the potentials of Refs. [27,28]. The curves represent the results of a four-parameter parametrization with $a_{0S}=19.69$ a.u., a_{0T}

$=64.57$ a.u., $C_6=1556$ a.u. [29], and $\Delta E_a^{HF}=1772$ MHz, where a_{0S} and a_{0T} are computed from the singlet and triplet potentials of Refs. [27,28]. Figure 1 shows the S -matrix element for the s -wave elastic scattering in channel $[\{F_1=1, F_2=1\}F=0, l=0, T=0]$. The feature around 130 mK is a Feshbach resonance in channel $[\{F_1=2, F_2=2\}F=0, l=0, T=0]$. For this particular case, $K^{c(LS)}$ is a 2×2 matrix:

$$K^{c(LS)} = \begin{pmatrix} K_S^c & 0 \\ 0 & K_T^c \end{pmatrix}, \quad (14)$$

with channel ordering shown in Table I. K_S^c and K_T^c are related to the singlet and triplet scattering lengths by Eq. (13). The frame transformation is given by [cf. Eqs. (11) and (12)]

$$U(T=0) = \frac{1}{2\sqrt{2}} \begin{pmatrix} \sqrt{3} & \sqrt{5} \\ \sqrt{5} & -\sqrt{3} \end{pmatrix}, \quad (15)$$

which leads to

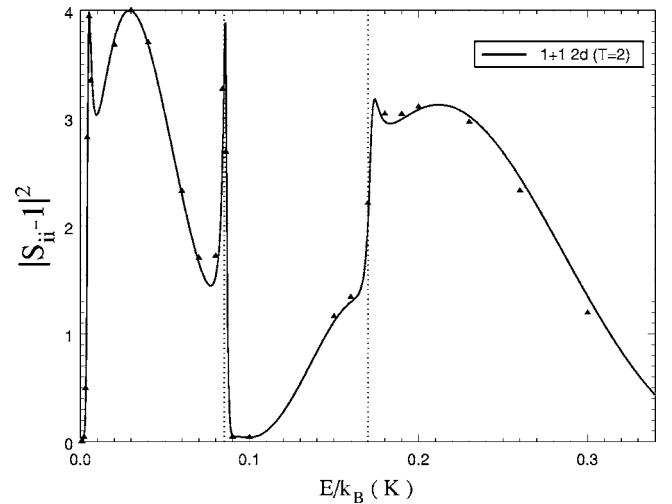


FIG. 2. The same as Fig. 1 except for d -wave channel $[\{F_1=1, F_2=1\}F=2, l=2, T=2]$.

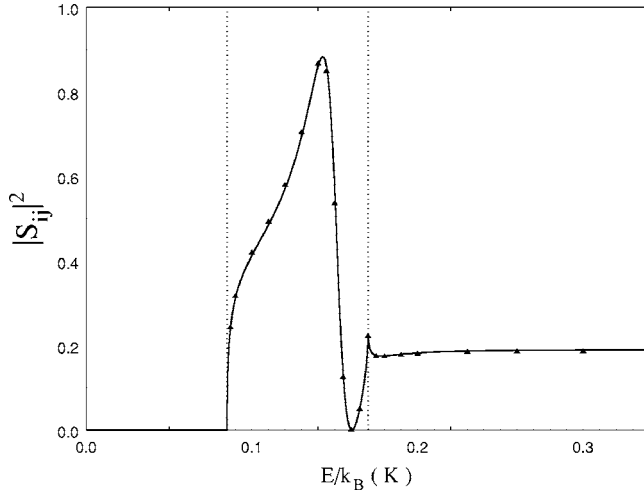


FIG. 3. The S -matrix element $|S_{ij}|^2$ for the s -wave inelastic scattering of two ^{23}Na atoms between channels $[\{F_1=1, F_2=1\}F=2, l=0, T=2]$ and $[\{F_1=1, F_2=2\}F=2, l=0, T=2]$.

$$K^c = \frac{1}{8} \begin{pmatrix} 3K_S^c + 5K_T^c & \sqrt{15}(K_S^c - K_T^c) \\ \sqrt{15}(K_S^c - K_T^c) & 5K_S^c + 3K_T^c \end{pmatrix}. \quad (16)$$

From the K^c matrix, the S matrix is obtained from the MAQDT equations (5)–(8). Note how Eq. (16) shows explicitly that the off-diagonal element of K^c , which determines the rate of inelastic collision due to exchange interaction, goes to zero for $K_S^c = K_T^c$ —namely, when $a_{0S} = a_{0T}$.

The results presented in Figs. 2 and 3 are obtained in similar fashion. Figure 2 shows the S -matrix element for the d -wave elastic scattering in channel $[\{F_1=1, F_2=1\}F=2, l=2, T=2]$. It illustrates how the same parameters that we use to describe the s -wave scattering also describe the d -wave scattering, due to the fact that K_S^c and K_T^c are insensitive to l [13,15]. Here the sharp features around the thresholds are d -wave shape resonances. Figure 3 shows the S -matrix element for the s -wave inelastic scattering between channel $[\{F_1=1, F_2=1\}F=2, l=0, T=2]$ and channel $[\{F_1=1, F_2=2\}F=2, l=0, T=2]$. The kinks (discontinuities in the derivative), in both Figs. 3 and 1 at the $\{F_1=2, F_2=2\}$ thresh-

TABLE I. Channel structure for s -wave scattering between two identical atoms with $L_1=L_2=0$, $S_1=S_2=1/2$, and $I_1=I_2=3/2$, in the absence of an external magnetic field. Examples include ^7Li , ^{23}Na , ^{39}K , and ^{87}Rb .

T	LS coupling (S, l)	FF coupling $\{F_1, F_2\}F$
0	$S=0, l=0$	$\{1, 1\}0$
	$S=1, l=1$	$\{2, 2\}0$
1	$S=1, l=1$	$\{1, 2\}1$
2	$S=0, l=2$	$\{1, 1\}2$
	$S=1, l=1$	$\{1, 2\}2$
	$S=1, l=3$	$\{2, 2\}2$
3	$S=1, l=3$	$\{1, 2\}3$
4	$S=1, l=3$	$\{2, 2\}4$

old, are general features associated with the opening of an s -wave channel. There is no kink at the $\{F_1=1, F_2=2\}$ threshold in Fig. 1 because the $[\{F_1=1, F_2=1\}F=0, l=0, T=0]$ channel is not coupled to $\{F_1=1, F_2=2\}$ channels.

The agreements between the MAQDT parametrization and close-coupling calculations are excellent, exact for all practical purposes, in all cases. Conceptually, these results illustrate that through a proper MAQDT formulation, collisions of alkali-metal atoms over a wide range of energies (300 mK compared to the Doppler cooling limit of about 0.2 mK for ^{23}Na), with complex structures including Feshbach and shape resonances and for different partial waves, can all be described by parameters that we often associate with the s -wave scattering at zero energy only—namely, the singlet and triplet scattering lengths. More generally, since the parameter that determines the energy variation of K^c around the threshold, β_8/β_6 , seems to have the same order of magnitude of around 1/2, or smaller, for all atoms, the same statement is expected to be applicable, over an energy range of hundreds to thousands of $(\hbar^2/2\mu)(1/\beta_6)^2$, to all atomic collisions with long-range interactions characterized by Eq. (3) with $n_i=6$. The theory can also be easily generalized to cover an even greater range of energies by incorporating the energy dependence of K^c into the parametrization.

V. CONCLUSION

In conclusion, a multichannel, angular-momentum-insensitive, quantum-defect theory for slow atomic collisions has been presented. We believe it to be the optimal formulation for purposes including exact numerical calculation, parametrization, and analytic representation. We have shown that by dealing with the short-range K matrix K^c , the frame transformation becomes basically exact, which greatly simplifies the description of any slow atomic collision with hyperfine structures. As an example, we have shown that even a simplest parametrization with four parameters, in which the energy and the l dependence of K_S^c and K_T^c are completely ignored, reproduces the close-coupling calculations for ^{23}Na atoms over a wide range of energies basically exactly. The effect of an external magnetic field, which is not considered in this article, is easily incorporated as it simply requires another frame transformation [10].

The concepts and main constructs of the theory can be generalized to other scattering processes including ion-atom scattering and atom-atom scattering in excited states. The key difference will be in the long-range interaction [cf. Eq. (3)]. In addition to possibly different long-range exponent n_i (such as $n_i=4$ for ion-atom scattering), there may also be long-range off-diagonal coupling that will have to be treated differently.

Finally, we expect that if we restrict ourselves to a smaller range of energies, of the order of $(\hbar^2/2\mu)(1/\beta_6)^2$ (about 1 mK for ^{23}Na), a number of analytic results, similar to the single-channel results of Refs. [5,6], can be derived even for the complex multichannel problem of alkali-metal collisions. These results may, in particular, lead to a more general and more rigorous parametrization of magnetic Feshbach reso-

nances (see, e.g., Refs. [12,30] for some recent works in this area).

ACKNOWLEDGMENT

B.G. was supported by the National Science Foundation under Grant No. PHY-0140295.

APPENDIX A: DEFINITIONS OF MAQDT FUNCTIONS

The reference functions f^c and g^c for a $-C_n/r^n$ ($n > 2$) potential are a pair of linearly independent solutions of the radial Schrödinger equation

$$\left[-\frac{\hbar^2}{2\mu} \frac{d^2}{dr^2} + \frac{\hbar^2 l(l+1)}{2\mu r^2} - \frac{C_n}{r^n} - \epsilon \right] u_{\epsilon l}(r) = 0, \quad (\text{A1})$$

which can be written in a dimensionless form as

$$\left[\frac{d^2}{dr_s^2} - \frac{l(l+1)}{r_s^2} + \frac{1}{r_s^n} + \epsilon_s \right] u_{\epsilon_s l}(r_s) = 0, \quad (\text{A2})$$

where $r_s = r/\beta_n$ is a scaled radius, $\beta_n \equiv (2\mu C_n/\hbar^2)^{1/(n-2)}$ is the length scale associated with the $-C_n/r^n$ interaction, and

$$\epsilon_s = \frac{\epsilon}{(\hbar^2/2\mu)(1/\beta_n)^2}, \quad (\text{A3})$$

is a scaled energy.

The f^c and g^c pair are chosen such that they have not only energy-independent, but also angular-momentum-independent behaviors in the region of $r \ll \beta_n$ (namely, $r_s \ll 1$):

$$f_{\epsilon_s l}^c(r_s) \underset{r_s \ll 1}{\sim} (2/\pi)^{1/2} r_s^{n/4} \cos(y - \pi/4), \quad (\text{A4})$$

$$g_{\epsilon_s l}^c(r_s) \underset{r_s \ll 1}{\sim} -(2/\pi)^{1/2} r_s^{n/4} \sin(y - \pi/4), \quad (\text{A5})$$

for all energies [13,24]. Here $y = [2/(n-2)]r_s^{-(n-2)/2}$. They are normalized such that

$$W(f^c, g^c) \equiv f^c \frac{dg^c}{dr_s} - \frac{df^c}{dr_s} g^c = 2/\pi. \quad (\text{A6})$$

For $\epsilon = 0$, the f^c and g^c pair for arbitrary n can be found in Ref. [15]. For $\epsilon \neq 0$, the f^c and g^c pair for $n=6$ can be found in Ref. [31]. They are related to the f^0 and g^0 pair of Ref. [16] by

$$\begin{pmatrix} f^c \\ g^c \end{pmatrix} = \frac{1}{\sqrt{2}} \begin{pmatrix} \cos(\pi\nu_0/2) & \sin(\pi\nu_0/2) \\ -\sin(\pi\nu_0/2) & \cos(\pi\nu_0/2) \end{pmatrix} \begin{pmatrix} 1 & 0 \\ 0 & -1 \end{pmatrix} \begin{pmatrix} f^0 \\ g^0 \end{pmatrix}, \quad (\text{A7})$$

where $\nu_0 = (2l+1)/4$ for $n=6$.

The $Z^{c(n)}(\epsilon_s, l)$ matrix is defined by the large- r asymptotic behaviors of f^c and g^c for $\epsilon > 0$,

$$f_{\epsilon_s l}^c(r_s) \underset{r \rightarrow \infty}{\sim} \sqrt{\frac{2}{\pi k_s}} \left[Z_{ff}^{c(n)}(\epsilon_s, l) \sin\left(k_s r_s - \frac{l\pi}{2}\right) - Z_{fg}^{c(n)}(\epsilon_s, l) \cos\left(k_s r_s - \frac{l\pi}{2}\right) \right], \quad (\text{A8})$$

$$g_{\epsilon_s l}^c(r_s) \underset{r \rightarrow \infty}{\sim} \sqrt{\frac{2}{\pi k_s}} \left[Z_{gf}^{c(n)}(\epsilon_s, l) \sin\left(k_s r_s - \frac{l\pi}{2}\right) - Z_{gg}^{c(n)}(\epsilon_s, l) \cos\left(k_s r_s - \frac{l\pi}{2}\right) \right], \quad (\text{A9})$$

where $k_s = k\beta_n$ with $k = (2\mu\epsilon/\hbar^2)^{1/2}$. This defines a 2×2 $Z^{c(n)}(\epsilon_s, l)$ matrix

$$Z^{c(n)} = \begin{pmatrix} Z_{ff}^{c(n)} & Z_{fg}^{c(n)} \\ Z_{gf}^{c(n)} & Z_{gg}^{c(n)} \end{pmatrix}. \quad (\text{A10})$$

It is normalized such that

$$\det[Z^{c(n)}] = Z_{ff}^{c(n)} Z_{gg}^{c(n)} - Z_{gf}^{c(n)} Z_{fg}^{c(n)} = 1. \quad (\text{A11})$$

The $\chi_l^{c(n)}(\epsilon_s)$ function is defined through the large- r asymptotic behaviors of f^c and g^c for $\epsilon < 0$:

$$f_{\epsilon_s l}^c(r_s) \underset{r \rightarrow \infty}{\sim} (2\pi\kappa_s)^{-1/2} [W_{f-}^{c(n)}(\epsilon_s, l) e^{\kappa_s r_s} - W_{f+}^{c(n)}(\epsilon_s, l) (2e^{-\kappa_s r_s})], \quad (\text{A12})$$

$$g_{\epsilon_s l}^c(r_s) \underset{r \rightarrow \infty}{\sim} (2\pi\kappa_s)^{-1/2} [W_{g-}^{c(n)}(\epsilon_s, l) e^{\kappa_s r_s} - W_{g+}^{c(n)}(\epsilon_s, l) (2e^{-\kappa_s r_s})], \quad (\text{A13})$$

where $\kappa_s = \kappa\beta_n$ with $\kappa = (2\mu|\epsilon|/\hbar^2)^{1/2}$. This defines a 2×2 $W^{c(n)}(\epsilon_s, l)$ matrix

$$W^{c(n)} = \begin{pmatrix} W_{f-}^{c(n)} & W_{f+}^{c(n)} \\ W_{g-}^{c(n)} & W_{g+}^{c(n)} \end{pmatrix}, \quad (\text{A14})$$

from which the $\chi_l^{c(n)}(\epsilon_s)$ function is defined by

$$\chi_l^{c(n)}(\epsilon_s) = W_{f-}^{c(n)}/W_{g-}^{c(n)}. \quad (\text{A15})$$

The $W^{c(n)}$ matrix is normalized such that

$$\det[W^{c(n)}] = W_{f-}^{c(n)} W_{g+}^{c(n)} - W_{g-}^{c(n)} W_{f+}^{c(n)} = 1. \quad (\text{A16})$$

The $Z^{c(n)}(\epsilon_s, l)$ and $W^{c(n)}(\epsilon_s, l)$ matrices, for $\epsilon > 0$ and $\epsilon < 0$, respectively, describe the propagation of a wave function in a $-C_n/r^n$ potential from small to large distances or vice versa. They are universal functions of the scaled energy ϵ_s with their functional forms determined only by the exponent n of the long-range potential and the l quantum number. The C_n coefficient and the reduced mass play a role only in determining the length and energy scales.

The $Z^{c(n)}$ matrix for $n=6$ is given in Ref. [14]. The $\chi_l^{c(n)}(\epsilon_s)$ function for $n=6$ is given in Ref. [13]. They are derived from Eq. (A7) and the asymptotic behaviors of the f^0 and g^0 pair given in Ref. [16].

APPENDIX B: K^c FROM NUMERICAL SOLUTIONS

Let $F(r)$ be the matrix, with elements $F_{ij}(r)$, representing any N linearly independent solutions of the close-coupling equation and $F'(r)$ be its corresponding derivative [Each column of $F(r)$ corresponds to one solution through Eq. (1).] For $r \geq r_0$, F can always be written as

$$F(r) = f^c(r)A - g^c(r)B, \quad (\text{B1})$$

where $f^c(r)$ and $g^c(r)$ are $N \times N$ diagonal matrices with diagonal elements given by $f_i^c(r)$ and $g_i^c(r)$, respectively. The matrices A and B can be obtained, e.g., from knowing $F(r)$ and $F'(r)$ at one particular $r \gg r_0$. Specifically,

$$A = (\pi\beta_n/2)[g^{c'}(r)F(r) - g^c(r)F'(r)], \quad (\text{B2})$$

$$B = (\pi\beta_n/2)[f^{c'}(r)F(r) - f^c(r)F'(r)]. \quad (\text{B3})$$

Comparing Eq. (B1) with Eq. (4) gives

$$K^c = [f^{c'}(r)F(r) - f^c(r)F'(r)][g^{c'}(r)F(r) - g^c(r)F'(r)]^{-1}. \quad (\text{B4})$$

In an actual numerical calculation, which can be implemented using a number of different methods [32], the right-hand side (RHS) of this equation is evaluated at progressively greater r until K^c converges to a constant matrix to a desired accuracy. This procedure also provides a numerical definition of r_0 ; namely, it is the radius at which the RHS of Eq. (B4) becomes an r -independent constant matrix.

-
- [1] W. C. Stwalley, Phys. Rev. Lett. **37**, 1628 (1976).
 [2] E. Tiesinga, B. J. Verhaar, and H. T. C. Stoof, Phys. Rev. A **47**, 4114 (1993).
 [3] J. Weiner, V. S. Bagnato, S. Zilio, and P. S. Julienne, Rev. Mod. Phys. **71**, 1 (1999).
 [4] J. M. Blatt and D. J. Jackson, Phys. Rev. **76**, 18 (1949).
 [5] B. Gao, Phys. Rev. A **58**, 4222 (1998).
 [6] B. Gao, J. Phys. B **37**, 4273 (2004).
 [7] F. H. Mies, Mol. Phys. **14**, 953 (1980).
 [8] P. S. Julienne and F. H. Mies, J. Opt. Soc. Am. B **6**, 2257 (1989).
 [9] B. Gao, Phys. Rev. A **54**, 2022 (1996).
 [10] J. P. Burke, Jr., C. H. Greene, and J. L. Bohn, Phys. Rev. Lett. **81**, 3355 (1998).
 [11] F. H. Mies and M. Raoult, Phys. Rev. A **62**, 012708 (2000).
 [12] M. Raoult and F. H. Mies, Phys. Rev. A **70**, 012710 (2004).
 [13] B. Gao, Phys. Rev. A **64**, 010701(R) (2001).
 [14] B. Gao, Phys. Rev. A **62**, 050702(R) (2000).
 [15] B. Gao, Eur. Phys. J. D **31**, 283 (2004).
 [16] B. Gao, Phys. Rev. A **58**, 1728 (1998).
 [17] B. Gao, Phys. Rev. A **59**, 2778 (1999).
 [18] A. R. P. Rau and U. Fano, Phys. Rev. A **4**, 1751 (1971).
 [19] C. M. Lee and K. T. Lu, Phys. Rev. A **8**, 1241 (1973).
 [20] C. M. Lee, Phys. Rev. A **11**, 1692 (1975).
 [21] M. J. Seaton, Rep. Prog. Phys. **46**, 167 (1983).
 [22] F. H. Mies, C. J. Williams, P. S. Julienne, and M. Krauss, J. Res. Natl. Inst. Stand. Technol. **101**, 521 (1996).
 [23] J. F. Babb and A. Dalgarno, Phys. Rev. Lett. **66**, 880 (1991).
 [24] B. Gao, J. Phys. B **36**, 2111 (2003).
 [25] H. T. C. Stoof, J. M. V. A. Koelman, and B. J. Verhaar, Phys. Rev. B **38**, 4688 (1988).
 [26] P. J. Leo, C. J. Williams, and P. S. Julienne, Phys. Rev. Lett. **85**, 2721 (2000).
 [27] C. Samuelis, E. Tiesinga, T. Laue, M. Elbs, H. Knöckel, and E. Tiemann, Phys. Rev. A **63**, 012710 (2000).
 [28] T. Laue, E. Tiesinga, C. Samuelis, H. Knöckel, and E. Tiemann, Phys. Rev. A **65**, 023412 (2002).
 [29] A. Derevianko, W. R. Johnson, M. S. Safronova, and J. F. Babb, Phys. Rev. Lett. **82**, 3589 (1999).
 [30] B. Marcellis, E. G. M. van Kempen, B. J. Verhaar, and S. J. J. M. F. Kokkermans, Phys. Rev. A **70**, 012701 (2004).
 [31] B. Gao, J. Phys. B **37**, L227 (2004).
 [32] G. H. Rawitscher, B. D. Esry, E. Tiesinga, J. P. Burke, Jr., and I. Koltracht, J. Chem. Phys. **111**, 10418 (1999).